# Rapid and reversible humidity-dependent colour change by water film formation in a scaled springtail

Bram Vanthournout, Frans Janssens, Gerben Debruyn, Johan Mertens, Karen De Clerck, Liliana D'Alba and Matthew Shawkey

INTERFACE

royalsocietypublishing.org/journal/rsif

Research

**Cite this article:** Vanthournout B, Janssens F, Debruyn G, Mertens J, Clerck KD, D'Alba L, Shawkey M. 2023 Rapid and reversible humidity-dependent colour change by water film formation in a scaled springtail. *J. R. Soc. Interface* **20**: 20230228.
https://doi.org/10.1098/rsif.2023.0228

Received: 19 April 2023
Accepted: 11 September 2023

**Subject Category:**
Life Sciences–Physics interface

**Subject Areas:**
biophysics

**Keywords:**
Collembola, humidity-dependent colour change, scale, spectrophotometry, optical modelling

**Author for correspondence:**
Matthew Shawkey
e-mail: matthew.shawkey@ugent.be

Electronic supplementary material is available online at https://doi.org/10.6084/m9.figshare.c.6845532.

THE ROYAL SOCIETY PUBLISHING

# Rapid and reversible humidity-dependent colour change by water film formation in a scaled springtail

Bram Vanthournout[1], Frans Janssens[3], Gerben Debruyn[1], Johan Mertens[2], Karen De Clerck[4], Liliana D'Alba[1,5] and Matthew Shawkey[1]

[1]Evolution and Optics of Nanostructures Group, Department of Biology and [2]Terrestrial Ecology Unit, Department of Biology, Ghent University, Ledeganckstraat 35, Ghent 9000, Belgium
[3]Department of Biology, University of Antwerp, Universiteitsplein 1, Wilrijk 2610, Belgium
[4]Centre for Textile Science and Engineering (CTSE), Ghent University, Technologiepark 70a, 9052 Zwijnaarde, Belgium
[5]Naturalis Biodiversity Center, Leiden, The Netherlands

BV, 0000-0001-6198-9092; GD, 0000-0002-6338-2865; LD, 0000-0002-2478-3455; MS, 0000-0002-5131-8209

Colour is often not a static trait but can change over time either through biotic or abiotic factors. Humidity-dependent colour change can occur through either morphological change (e.g. to feather barbules in birds) or by the replacement of air by water causing a shift in refractive index, as seen in arthropod multi-layer cuticles or scales. The scaled springtail *Lepidocyrtus cyaneus* has scales that produce colour largely via thin film interference from their lamina. We observed a marked colour change from golden to violet/purple coloration in humid conditions. Light microscopy, micro-spectrophotometry, contact angle goniometry and optical modelling indicate that the formation of a thin film of water on top of the hydrophilic scales increases their laminar thin film thickness, causing a shift towards violet/purple colour. Evaporation of the water film causes the metallic golden colour to return. This constitutes a remarkably rapid colour change (in the order of seconds), only limited by the speed of water film condensation and evaporation, that may serve as inspiration for new dynamically coloured materials and sensors.

## 1. Introduction

Colour can be produced by pigments whose chemical structures cause selective absorption of certain wavelengths, or by periodic biophotonic nanostructures causing coherent light scattering and producing (typically) iridescent structural coloration. Though the colour of an organism is often fixed during its lifetime, spectacular examples of dynamic colour change exist that play a role in camouflage [1] and inter- and intra-species communication [2]. These active colour changes, often a combination of both pigmentary and structural coloration, can be caused by the slow migration [3] or formation of pigment granules [4], the rapid expansion and contraction of chromatophores [5,6] and the active expulsion of liquid in the multi-layer of the cuticle [7]. Passive changes, not requiring an action of the organism, are often initiated by abiotic factors, such as humidity, and are generally found in structural colours. In the mourning dove, *Zenaida macroura*, an increase in reflectance was caused by a twisting of feather barbules upon wetting [8], while in the tree swallow *Tachycineta bicolor*, swelling of the outer keratin layer results in a rapid colour change in iridescent feathers [9]. In *Dynastes* beetles, the elytra cuticle contains a porous yellow spongy layer that functions as a photonic crystal. In the yellowish green-coloured dry state, the cavities of this spongy layer are filled with air while water accumulates with wetting. This results in a change in refractive index (RI) contrast (RI air = 1, RI water = 1.33, $\Delta n = 0.33$), which reduces the backscattering of the spongy layer and exposes the dark cuticle underneath, and results in a black coloration of the elytra [10–12]. A change in refractive index contrast between the interfaces in a multi-layer in the cuticle causing a colour change can also be found in the seaweed *Chondrus crispus* under wet and dry conditions [13]. A similar mechanism, where the replacement of air by water causes changes in the refractive index, is found in the multi-layer scales on the wings of *Morpho* butterflies [14] and green forester moths (*Adscita statices*) [15] and in the scales of the beetle *Hoplia coerulea* [16]. In the longhorn beetle, *Tmesisternus isabellae* both swelling of the multi-layer period in the scale and refractive index contrast reduction due to water infiltration leads to a marked colour change [17].

We observed that laboratory-reared scaled springtails *Lepidocyrtus cyaneus* Tullberg 1871 (Collembola), changed from golden to violet/purple colours when crossing areas of low and high humidity (dry and wet plaster at the bottom of the rearing container), respectively. This change was instantaneous and reversible (B.V., personal observation), but the mechanism was not obvious.

Metallic coloration in arthropods can be caused by a chirped multi-layer in beetle elytra [18] and by a pigmented scale lamina on the wings of micromoths [19]. The metallic coloration of body scales of Collembola has a similar origin as the latter example, as collembolan scales are characterized by a fused chitin lamina adorned with interrupted, sail-like spinulate ridges that contain melanin (figure 3*e–g*) [20]. The broadband metallic coloration in *L. cyaneus* mainly results from the unpigmented scale lamina acting as a thin film and, to a lesser extent, from the diffraction grating effects of the ridges [20]. Microscale variation in scale thickness and ridge dimensions generates a patchy distribution of colours (including gold and silver) and results, through spatial colour mixing, in a metallic coloration when viewed on a larger scale [20]. As these scales are non-porous and simply structured, we hypothesized that colour change occurred via a swelling of the scale through water absorption that increases the scale lamina thickness and the ridge dimension, or by the formation of a water film between the ridges, which might interact with the thin film and diffraction grating colour production dynamics.

To test this hypothesis, we first investigated this process using light microscopy, quantified scale colour by microspectrophotometry, determined scale wettability using contact angle goniometry and explored the potential underlying mechanisms (i.e. scale expansion and water film formation) using finite-difference time-domain (FDTD) optical modelling.

# 2. Material and methods

## 2.1. Sample collection

*Lepidocyrtus cyaneus* individuals were collected using a hand vacuum cleaner in a lawn in a private garden in Belgium (51.094148° N, 3.065399° E) in early December 2022 and kept in laboratory conditions [20]. Scanning electron microscopy (SEM) and transmission electron microscopy (TEM) pictures originated from a laboratory-reared population at Ghent University [20] and were taken in December 2017 and 2018, respectively.

## 2.2. Scale morphology

For SEM, an entire individual was mounted ventral-side-down on an aluminium stub using double-sided carbon tape and coated with Au/Pd. Dorsal scales were viewed on a field emission gun (FEG)-SEM (FEI Quanta 200F, The Netherlands) under an accelerating voltage of 10 kV and a working distance of 9.5 mm.

For TEM, entire individuals were embedded following the protocol described in [21]. Briefly, samples undergo two dehydration steps using 100% ethanol (20 min) and go through an infiltration series with 15, 50, 70 and 100% Epon (24 h each step). Next, infiltrated individuals were placed in block moulds and polymerized for 16 h at 60°C. Thin cross-sections (100 nm) were cut using a Leica UC-6 ultramicrotome (Leica Microsystems, Germany). Cross-sections were stained in a Uranyless/lead citrate solution and examined on a JEOL JEM 1010 (Jeol, Ltd, Tokyo, Japan) transmission electron microscope.

## 2.3. Scale coloration and humidity treatment.

We investigated the humidity-dependent colour change by placing a freshly dead (after deep freezing) individual of *L. cyaneus* on a dry black paper substrate and wetting the substrate with tap water using a pipette until saturation. Colour change was observed through a Leica M80 stereomicroscope. We repeated this procedure using a natural background (sand substrate on which the individuals were collected) to observe the colour change on a relevant natural background.

We quantified the colour of dry and wet scales on a glass slide by measuring the specular reflectance in the visible spectrum (400–700 nm) of the dorsal scale surface. We used a CRAIC AX10 UV–Visible micro-spectrophotometer (CRAIC Technologies, Inc., USA) with a 50× objective (numerical aperture 0.7 and integration time of 440.54 and 607.76 ms) and a 75 W Xenon short arc lamp (Ushio UXL-75XE) as a light source. White and black standards (Avantes Reference Tiles WS-2) were used as reference for calibration. Images and videos were acquired using the PixeLINK 1.3 Megapixel FireWire Camera on standard settings. To quantify the speed of the colour change, we determined time points of colour change in Windows Video Editor. A humidity treatment was provided by misting the scales with a humidifier (Samsung Ultrasonic Humidifier, HU-3850DW, set at 70% humidity) with an attached rubber hose to control misting direction and concurrently measuring the reflectance or taking pictures.

## 2.4. Scale wettability

We tested the wettability of the scaled dorsal surface of a *L. cyaneus* individual with contact angle goniometry, using an OCA 25 contact angle set-up from DataPhysics. By performing the sessile drop method, we observed the extent of drop adherence to the scales (see [22] for an example of drop behaviour on Collembola cuticle). Drops on a hydrophobic surface maintain their round shape while drops on a hydrophilic surface demonstrate clear adherence. We further quantified the contact angle of a deionized water droplet placed on the scales at room conditions (25°C, (30 ± 10)% relative humidity). As the sessile drop method was only successful in generating smaller drops without fully submerging the animal, we additionally used a spray bottle to deposit larger drops. We measured the initial contact angle three times per drop with ImageJ (v. 1.53o) software [23]. By definition, a surface can be viewed as hydrophilic ($\theta c < 90°$), hydrophobic ($\theta c > 90°$) and super hydrophobic ($\theta c > 150°$).

## 2.5. Optical modelling

We constructed a simplified three-dimensional model (SketchUp (Trimble Inc.)) of a *L. cyaneus* scale based on previous morphological measurements ([20], figure 1) with scale thickness (130 nm), ridge base (200 nm), ridge height (200 nm), ridge distance (600 nm) and ridge length (2000 nm). We constructed models consisting of only ridges, only the scale lamina and a combination of lamina + ridges (figure 1) to individually assess the contribution

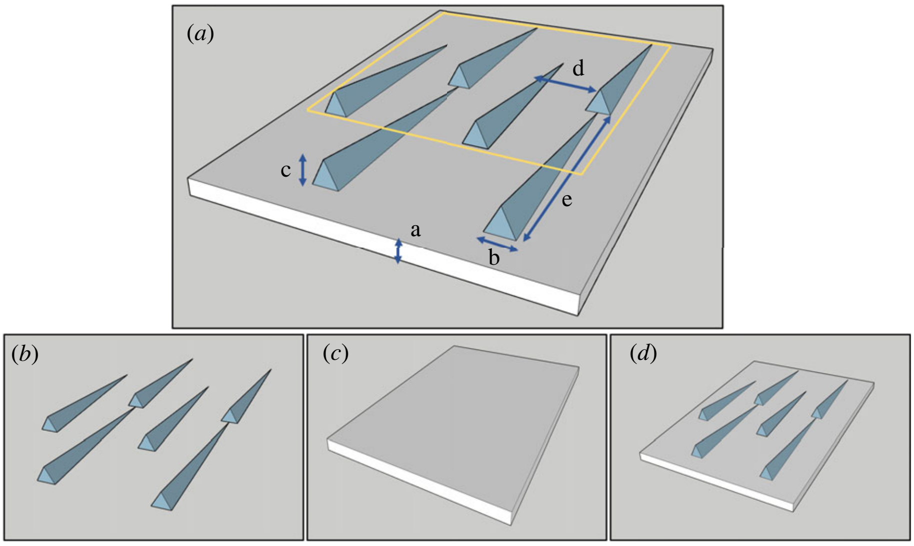


**Figure 1.** (*a*) Simplified three-dimensional model of a *L. cyaneus* scale with scale thickness a, ridge base b, ridge height c, ridge distance d and ridge length e, with indication of the simulation area (yellow lines). Ridge-only (*b*), lamina-only (*c*) and lamina+ridge models (*d*) used in FDTD simulations.

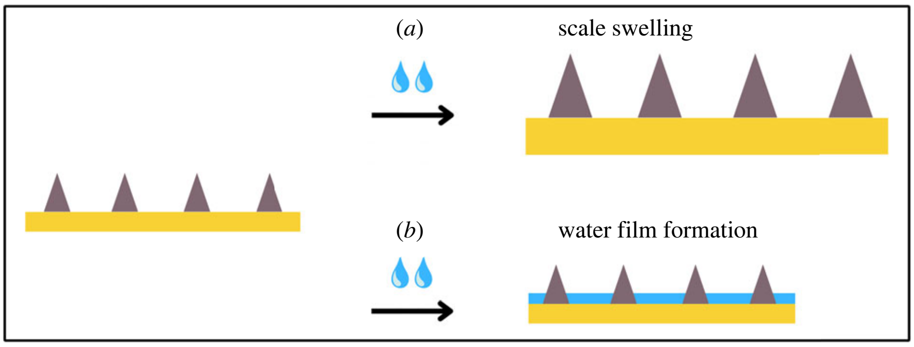


**Figure 2.** Two tested mechanisms for humidity-dependent colour change in *L. cyaneus*. (*a*) Scale swelling might result from the absorption of water and results in an increase in lamina thickness and ridge size. (*b*) Water might accumulate between the ridges and form a water film.

of these structures to the colour change according to the following scenarios (figure 2).

To test if the colour change is caused by the absorption of water and consequent swelling of the scale, resulting in an increase in scale thickness and ridge dimensions, we created ridge-only, lamina-only and lamina+ridge models (figure 1) of varying dimensions by rescaling by 5, 10, 15, 20, 30 and 40% in SketchUp.

Alternatively, to investigate whether the colour change could be caused by the formation of a water film between the ridges that interacts with the scale lamina thin film, we added water layers with varying thickness (20, 50, 75, 100, 150, 200, 400, 600, 800 and 1000 nm) to the lamina and lamina + ridge models. As simulations show that the ridges have no effect when completely covered with water (see further), we used lamina-only models for water layer thicknesses of more than 200 nm. Additionally, we also investigated the effect of only a water film (water film-only, no scale lamina or ridges) by simulating reflectance spectra for water films with varying thickness (20, 50, 75, 100, 150, 200, 400, 600, 800 and 1000 nm).

We performed FDTD modelling using a commercial Maxwell equation solver (Ansys-Lumerical Solutions, Ansys Canada Ltd) with the lamina and ridges consisting of chitin and melanin [20], respectively. Refractive indices of chitin and melanin were taken from previous studies [24,25], we used the already available refractive index value of water (RI = 1.33) in the Ansys-Lumerical software. We used perfectly matched layers [26] to absorb electromagnetic waves on the bottom and top of the simulation area, while periodic boundary conditions were used on the side to simulate infinite periodic structures. The light source ranged from 300 to 750 nm and consisted of an unpolarized plane wave with normal incidence.

Simulated and experimental reflectance spectra were visualized using the pavo package [27] in RStudio [28] (v. 4.1.2).

# 3. Results

## 3.1. Humidity-dependent colour change

The observed colour change from a broadband metallic golden colour to violet purple and back to gold is a rapid, reversible process and occurs instantaneously upon increasing humidity through wetting of the substrate or misting of scales with water vapour (figures 3 and 4; electronic supplementary material, figure S1 and videos S1, S2a and S2b). The colour change reverses back to metallic golden when misting is stopped and occurs in intact animals as well as in individual scales. When single scales are observed in detail, coloured patches show a clear shift towards longer wavelengths resulting in golden patches (with increasing reflectance towards longer wavelengths) shifting to a clear violet/blue colour (reflectance peak at 465, 471 and 440 nm for figure 6*a*, 6*b* and 6*c*, respectively, see also figure 4 and electronic supplementary material, video 2a and 2b).

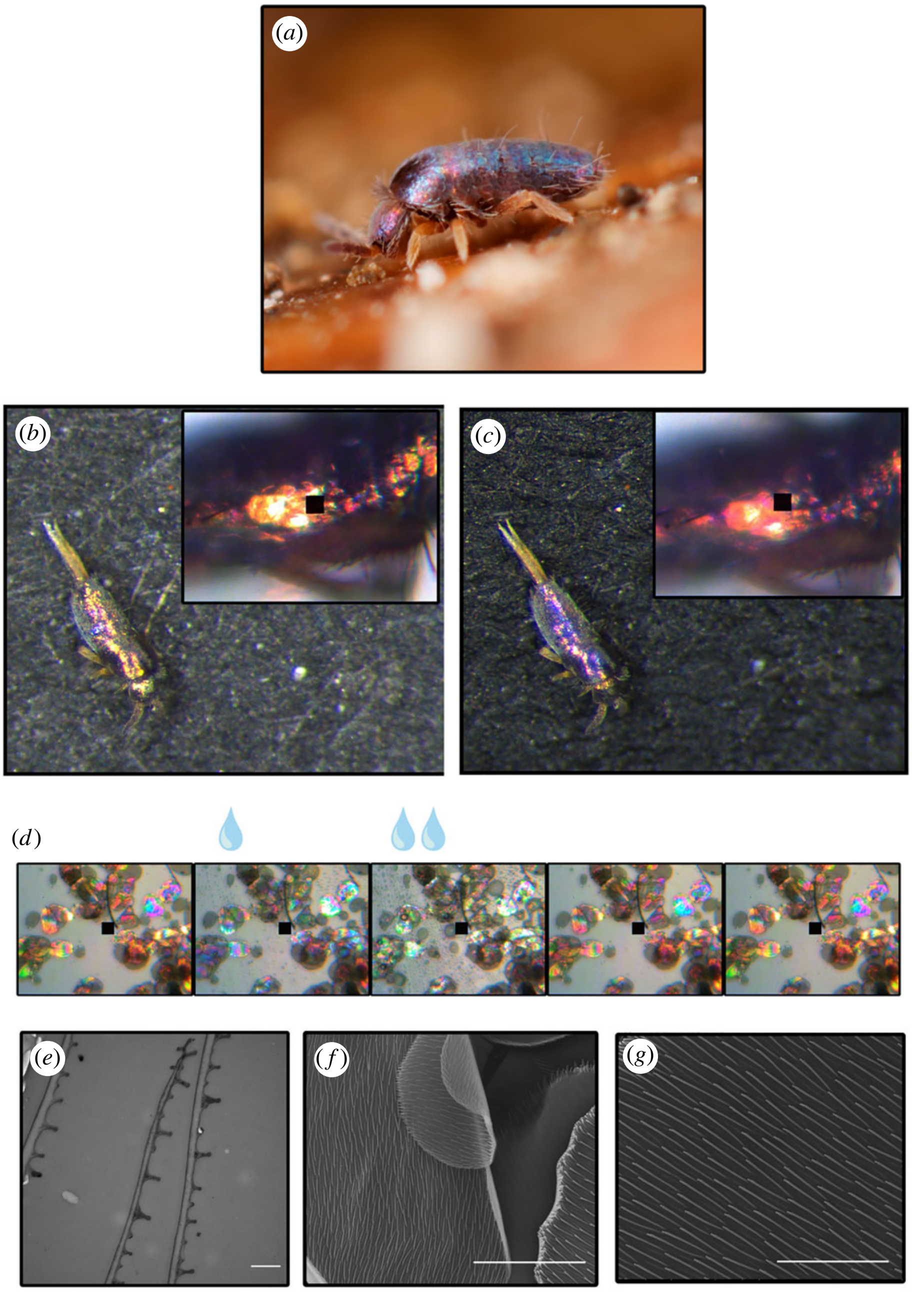


**Figure 3.** Habitus picture of *L. cyaneus* showing the violet coloration (© Marie Louise Huskens) (*a*). Colour change from metallic golden to purple/violet, before (*b*) and after (*c*) wetting of the substrate with water. Animal length is approximately 1.5 mm, based on literature [29]. Inserts show a magnified image of the dorsal part of the abdomen of another individual before and after misting. Time series of wetting and drying (*d*) (indicated by number of drops) of scales on a glass slide by misting with water vapour, showing reversible colour changes in individual scales. TEM picture (*e*) of a cross-section of scales showing scale lamina and ridges. SEM pictures (*f*,*g*) of dorsal scale ultrastructure with herringbone pattern of ridges (picture (*g*) reproduced from Vanthournout *et al*. [20]). The black square in (*b*–*d*) represents the probe measuring area of the micro-spectrophotometer with sides measuring 15 × 15 µm. Scales in (*e*–*g*) indicate 400 nm, 10 µm and 5 µm, respectively.

This is not limited to golden patches as a red shift (towards longer wavelengths) also occurs for patches with a different starting colour (e.g. green, etc.) in the dry state. Original (pre-misting) colours are restored upon drying, although the reflectance is possibly somewhat lower. This process takes around 1 s to complete (electronic supplementary material, videos S2a and 2b). In electronic supplementary material, video S2b, six cycles of colour change are recorded in under 20 s. Upon start of misting, average time to go from golden to bluish colour per cycle is 0.88 ± 0.10 s (mean ± s.e.), while cessation of misting returns a golden colour in 1.3 ± 0.07 s (mean ± s.e., see electronic supplementary material, table S1). Increasing humidity levels by misting for longer than 3 s (figures 4 and 6*c*; electronic supplementary material, video S3) generate a highly patchy and banded distribution of colours, resulting in reflectance spectra with multiple peaks. The water drop behaviour from the contact angle goniometer (figure 5*a*) shows clear adherence of the droplet on the scale surface. The hydrophilic nature of the scales is further confirmed by the contact angle for a drop using the sessile drop method (average ± s.d., 47.75° ± 2.2°, electronic supplementary material, figure S2) and for a drop originating from spraying (62.31° ± 3.3°, figure 5*b*) as both are well below the hydrophobic 90° cut-off. Moreover, droplets disappear quickly after deposition, indicating rapid evaporation or a spreading over neighbouring scales (electronic supplementary material, videos S5 and S6).

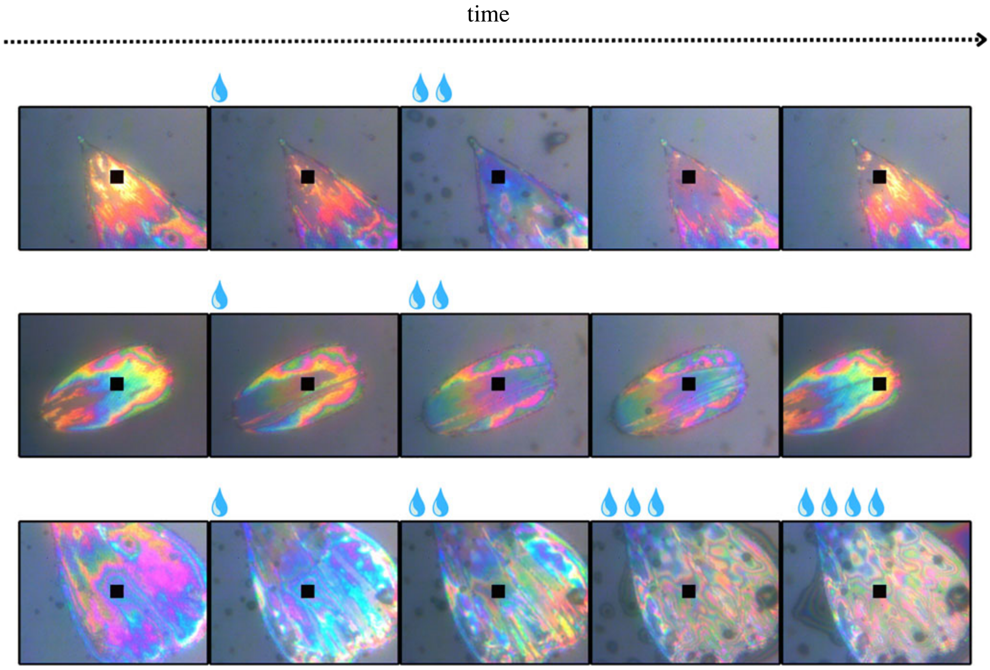


**Figure 4.** Wetting and drying time series of *L. cyaneus* scales on a glass slide with the extent of wetting indicated by number of water drops. First picture shows the initial dry state, the two last pictures show the dry state after water evaporation (for first two rows), while for the last row misting continued to achieve excessive wetting. The black square represents the measuring area of the micro-spectrophotometer probe with sides of 3 × 3 µm.

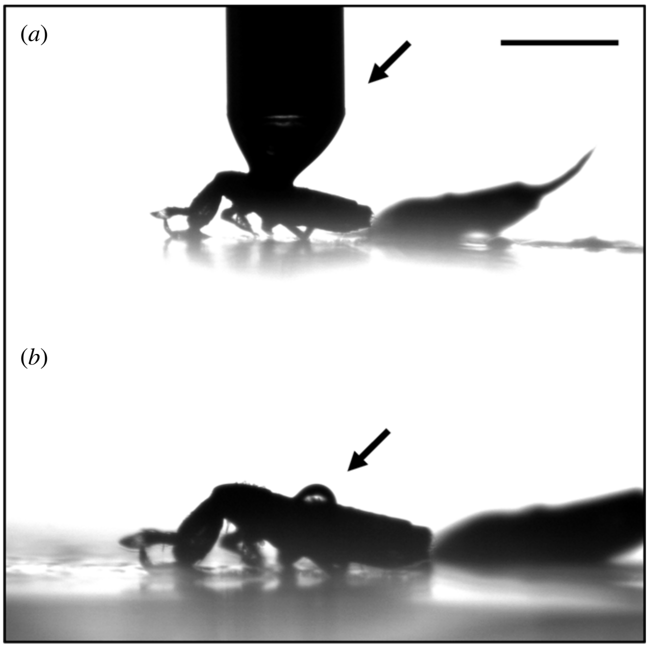


**Figure 5.** Image from contact angle goniometer (needle indicated by an arrow) showing an adhered water droplet (*a*) and a deposited water droplet (indicated by an arrow) by spraying (*b*) on the dorsal surface of an *L. cyaneus* individual. Scale bar depicts 0.5 mm.

## 3.2. Optical modelling

To identify the mechanism underlying the rapid colour change in *L. cyaneus*, we performed FDTD modelling of the hypothesized scale swelling and water film formation scenarios. For the scale expansion scenario, simulation results of the lamina and lamina + ridge models indeed show a red shift with increasing scale dimensions (thicker lamina and larger ridges) that are consistent with the observed experimental spectra. The ridge model consistently returns spectra with multiple peaks across the entire spectrum (electronic supplementary material, figure S3). However, it is unlikely that scale expansion by water absorption plays a large role in the colour change, as a size increase of at least 40% is needed to generate a bluish colour (electronic supplementary material, figure S3a) and no apparent visual changes to scale dimensions were observed during the misting process (readjustment of the focus was not required). On the other hand, simulating the formation of a thin water film on top of the scale also results in a clear red shift for the lamina-only (figure 6*d*) model. A water film of 50 and 75 nm generates a peak in the violet and purple region, while thicker water films (100 and 150 nm) generate peaks in the blue and green region. For the lamina + ridge model (figure 6*e*), thinner water films of 20, 50 and 75 nm resulted in broad reflectance spectra with multiple peaks in the blue/green and red region while films of 100 and 150 nm produced clear peaks in the blue and green region. Not surprisingly, the ridges (200 nm height) have the largest effect on colour when simulating water film thicknesses less than or equal to 75 nm (electronic supplementary material, figure S4) as this leaves part of the ridge exposed causing a general dampening effect resulting in a broad reflectance across the spectrum (figure 6*e*). As the thickness of the water layer increases, the effect of the ridges is reduced until a water layer thickness of 200 nm, leaving the ridges completely submerged and therefore not contributing to reflectance (identical spectra for lamina-only and lamina + ridge models, see electronic supplementary material, figure S4). For this reason, we limited simulations of a water layer of 200 nm or more to the lamina-only model. These predict spectra with an increasing number of peaks (figure 6*f*), in agreement with the occurrence of multi-colour bands in scales with high levels of humidity (figure 6*c*).

To investigate the contribution of the water film, we simulated the reflectance spectra for water film-only models with varying thickness (electronic supplementary material, figure S5). These show that the water film on its own is unlikely to produce the colour change, as smaller thicknesses

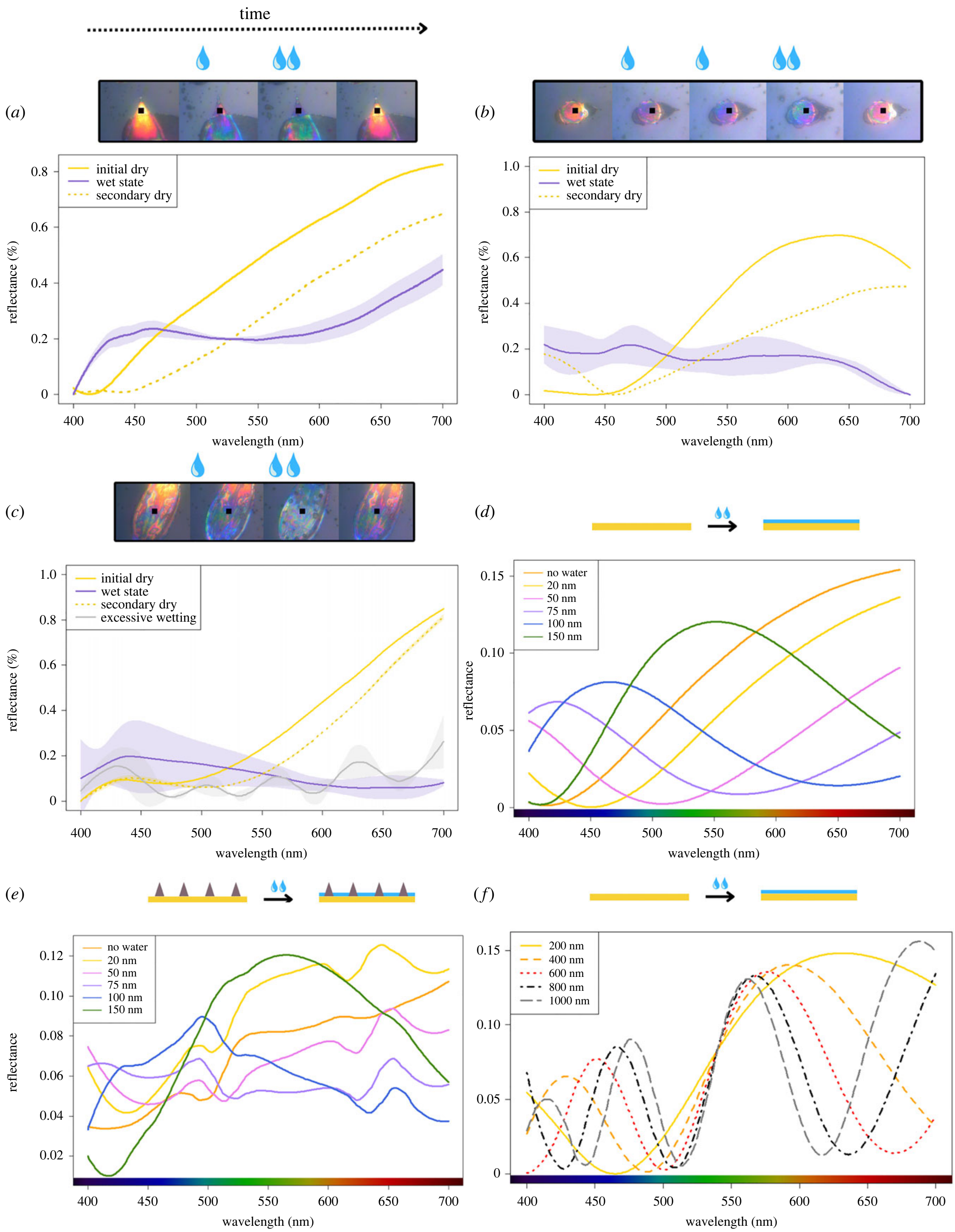


**Figure 6.** Image sequence of dry and wet scales with the degree of misting indicated by the number of water drops (first and last picture showing the dry state) and corresponding normalized experimental reflectance spectra (*a–c*). In the dry state, scales exhibit a golden metallic colour (gold solid line, mean ± 95% s.d.), while after wetting, the spectrum displays a shift towards purple/violet coloration (violet solid line). After drying, the golden metallic colour is returned (golden dashed line). Upon excessive wetting (*c*), the scale exhibits a patchy colour appearance resulting in a spectrum with multiple peaks (solid grey line). Reflectance spectra resulting from optical simulations of a water film of varying thickness on the scale lamina (*d*,*f*) and on the lamina + ridge model (*e*).

produce spectra without clear peaks. Rather, the additive effect of the water film thickens the scale lamina and thus changes the generated colour.

A likely water film forms in the direction of the longitudinal ridges during misting (figure 4; electronic supplementary material, video S4). This water layer may darken scale colour, consistent with the dampening effect of thin water films (less than 100 nm) in the lamina + ridge models (figure 6*e*).

## 4. Discussion

We investigated rapid and reversible humidity-dependent colour change in the springtail *L. cyaneus*. Though also visible when attached to the body, we confirmed this change occurs at the level of individual scales. Wetting markedly shifts reflectance towards higher wavelengths, causing golden spots to exhibit a violet/purple hue. Upon drying, the scales again turn golden. This process is reversible and takes only a few seconds. Using optical modelling, we showed that this probably occurs via the formation of a water film between the ridges. Scale swelling has been observed in the longhorn beetle *Tmesisternus isabellae* [17] but is unlikely to significantly contribute to the colour change in *L. cyaneus*, as simulations indicate that an expansion of at least 40% is required to produce a blue coloration (electronic supplementary material, figure S3) and we observed no obvious changes in scale dimensions during wetting and drying. Rather, the formation of a water film is consistent with the observed colour change and simulations show that a chromatic colour is obtained with a water film of 50 and 75 nm (figure 6*d*) in the lamina-only model. Larger water layers of 100 and 150 nm produce the blue and green colours. Simulating even thicker water layers results in reflectance spectra with multiple peaks, consistent with the banded colours that are observed after excessive wetting (figure 6*e*).

The metallic golden coloration of *L. cyaneus* is mainly determined by thin film effects originating from the thickness of the scale lamina [20], but ridge effects cannot be ruled out. This is consistent with our simulation results, which indicate that the lamina thickness is the main cause of the colour change. The formation of a water film on top of the scale effectively increases this thickness and generates a colour shift. The ridges seem to, at most, dampen colour (figure 6*e*). Not surprisingly, this ridge effect is only apparent when water films are simulated that are smaller than the ridge height (electronic supplementary material, figure S4) and could be consistent with the appearance of darker colours at the onset of water film condensation (figure 4; electronic supplementary material, video S4).

While the function of the scales in Collembola has been shown to be anti-predatory [30], the role (if any) of the colour change is not clear for *L. cyaneus*. It may function as dynamic camouflage as humid areas are characterized by a darker background (darker soil due to higher water content, the presence of plants that blocks light [31]) and dryer areas are often paler. Rapidly switching between a violet/purple and golden colour could enable stronger background matching (see also electronic supplementary material, figure S1) though it is crucial to determine the role of visual hunting in collembolan predators [32–35]. Alternatively, the scales could counter dehydration by trapping a layer of water around the animal. To achieve this, the hydrophilic nature of the scales could work in tandem with the highly hydrophobic integument [36], but this remains to be tested. In this way, the colour change could also be a non-adaptive side-effect of scale morphology and hydrophilicity. Further testing of the camouflage and dehydration hypotheses is therefore required to unambiguously assign any biological relevance to the observed colour change.

The formation of a water film is loosely comparable to the already known mechanism of colour change in porous, multilayered scales [14–17], as the replacement of air by water might also induce the formation of a water thin film. Its speed, however, is fundamentally different, taking only seconds to complete whereas the process in multi-layer scales generally takes minutes. This may be because the basal structure of the collembolan scale, consisting of a fused basal lamina and longitudinal ridges, allows formation of the water film on top of the lamina. This process is rapid, as it is not hampered by infiltration processes but limited only by the speed of water film condensation and subsequent evaporation. As such, the formation of a water film on top of a scale constitutes a novel mechanism of rapid colour change. Interestingly, the colour change in the feathers of the tree swallow *Tachycineta bicolor* also occurs in seconds yet employs a different mechanism of keratin swelling [9].

We did not determine the sensitivity of water film formation for different humidity levels, but we assume that a low humidity threshold is required, as wetting of the substrate is sufficient to initiate a colour change (figure 3*b*,*c*). Both the sensitivity and the speed of water film formation are probably increased by the hydrophilic nature of the scales (figure 5). Further quantification of the scales' hydrophilic capabilities, including the role of the spinulate ridges, and exploration of the potential of this design for biomimetic humidity sensors [37] and fog harvesting devices [38], are exciting avenues for future research. Moreover, expanding this research to include other scaled Collembola that have continuous longitudinal ridges (i.e. Tomoceridae) and other scaled groups such as Zygentoma and Archaeognatha would give even more insight into how scale morphology might relate to hydrophilicity and ultimately might lead to the identification of other examples of humidity-dependent colour change. The accidental discovery of colour plasticity in *L. cyaneus* underscores the need to also examine small organisms closely (*L. cyaneus* body size is max 1.5 mm [29]), as their colour change is less obvious and might more easily go undetected.

Ethics. This work did not require ethical approval from a human subject or animal welfare committee.

Data accessibility. All raw data and R code has been made available as electronic supplementary material. Videos of image compilations and video recordings can be accessed on from the Dryad Digital Repository: https://doi.org/10.5061/dryad.w0vt4b8z7.

The data are provided in the electronic supplementary material [39].

Declaration of AI use. We have not used AI-assisted technologies in creating this article.

Authors' contributions. B.V.: conceptualization, data curation, formal analysis, methodology, software, visualization, writing—original draft and writing—review and editing; F.J.: conceptualization, methodology and writing—review and editing; G.D.: conceptualization, formal analysis, methodology and writing—review and editing; J.M.: conceptualization, methodology and writing—review and editing; K.D.C.: conceptualization, funding acquisition, methodology, resources and writing—review and editing; L.D.: conceptualization, funding acquisition, methodology, supervision and writing—review and editing; M.S.: conceptualization, funding acquisition, methodology, resources, supervision and writing—review and editing.

All authors gave final approval for publication and agreed to be held accountable for the work performed therein.

Conflict of interest declaration. We declare we have no competing interests.

Funding. We acknowledge support from the UGent Special Research Fund, from the USA Air Force Office of Scientific Research (AFOSR FA9550-18-1-0477 to M.S.) and from the Research Foundation, Flanders (FWO G0A7921N to M.S. and K.D.C.).

Acknowledgements. We wholeheartedly thank Marie Louise Huskens for the use of the *L. cyaneus* habitus picture.

# References


1. Chittka L. 2001 Camouflage of predatory crab spiders on flowers and the colour perception of bees (Aranida: Thomisidae/Hymenoptera: Apidae). *Entomol. Generalis* **25**, 181–187. (doi:10.1127/entom.gen/25/2001/181)
2. Mathger LM, Denton EJ, Marshall NJ, Hanlon RT. 2009 Mechanisms and behavioural functions of structural coloration in cephalopods. *J. R. Soc. Interface* **6**, S149–SS63. (doi:10.1098/rsif.2008.0366.focus)
3. Filshie BK, Day MF, Mercer EH. 1975 Colour and colour change in the grasshopper, *Kosciuscola tristis*. *J. Insect Physiol.* **21**, 1763–1770. (doi:10.1016/0022-1910(75)90238-3)
4. Insausti TC, Casas J. 2008 The functional morphology of color changing in a spider: development of ommochrome pigment granules. *J. Exp. Biol.* **211**, 780–789. (doi:10.1242/jeb.014043)
5. Williams TL *et al.* 2019 Dynamic pigmentary and structural coloration within cephalopod chromatophore organs. *Nat. Commun.* **10**, 1004. (doi:10.1038/s41467-019-08891-x)
6. Mathger LM, Bell GRR, Kuzirian AM, Allen JJ, Hanlon RT. 2012 How does the blue-ringed octopus (*Hapalochlaena lunulata*) flash its blue rings? *J. Exp. Biol.* **215**, 3752–3757. (doi:10.1242/jeb.076869)
7. Vigneron JP *et al.* 2007 Switchable reflector in the Panamanian tortoise beetle *Charidotella egregia* (Chrysomelidae: Cassidinae). *Phys. Rev. E* **76**, 031907. (doi:10.1103/PhysRevE.76.031907)
8. Shawkey MD, D'Alba L, Wozny J, Eliason C, Koop JAH, Jia L. 2011 Structural color change following hydration and dehydration of iridescent mourning dove (*Zenaida macroura*) feathers. *Zoology* **114**, 59–68. (doi:10.1016/j.zool.2010.11.001)
9. Eliason CM, Shawkey MD. 2010 Rapid, reversible response of iridescent feather color to ambient humidity. *Opt. Express* **18**, 21 284–21 292. (doi:10.1364/OE.18.021284)
10. Hinton HE, Jarman GM. 1972 Physiological colour change in the Hercules beetle. *Nature* **238**, 160–161. (doi:10.1038/238160a0)
11. Rassart M, Colomer JF, Tabarrant T, Vigneron JP. 2008 Diffractive hygrochromic effect in the cuticle of the hercules beetle *Dynastes hercules*. *New J. Phys.* **10**, 033014. (doi:10.1088/1367-2630/10/3/033014)
12. Sun J, Wu W, Tian L, Li W, Zhang F, Wang Y. 2021 Investigation of the selective color-changing mechanism of *Dynastes tityus* beetle (Coleoptera: Scarabaeidae). *Sci. Rep.* **11**, 808. (doi:10.1038/s41598-020-80699-y)
13. Chandler CJ, Wilts BD, Vignolini S, Brodie J, Steiner U, Rudall PJ, Glover BJ, Gregory T, Walker RH. 2015 Structural colour in *Chondrus crispus*. *Sci. Rep.* **5**, 11645. (doi:10.1038/srep11645)
14. Potyrailo RA, Ghiradella H, Vertiatchikh A, Dovidenko K, Cournoyer JR, Olson E. 2007 Morpho butterfly wing scales demonstrate highly selective vapour response. *Nat. Photonics* **1**, 123–128. (doi:10.1038/nphoton.2007.2)
15. Wilts BD, Mothanderz K, Kelber A. 2019 Humidity-dependent colour change in the green forester moth, *Adscita statices*. *Biol. Lett.* **15**, 20190516. (doi:10.1098/rsbl.2019.0516)
16. Rassart M, Simonis P, Bay A, Deparis O, Vigneron JP. 2009 Scale coloration change following water absorption in the beetle *Hoplia coerulea* (Coleoptera). *Phys. Rev. E* **80**, 031910. (doi:10.1103/PhysRevE.80.031910)
17. Liu F, Dong BQ, Liu XH, Zheng YM, Zi J. 2009 Structural color change in longhorn beetles *Tmesisternus isabellae*. *Opt. Express* **17**, 16 183–16 191. (doi:10.1364/OE.17.016183)
18. Campos-Fernandez C, Azofeifa DE, Hernandez-Jimenez M, Ruiz-Ruiz A, Vargas WE. 2011 Visible light reflection spectra from cuticle layered materials. *Opt. Mater. Express* **1**, 85–100. (doi:10.1364/OME.1.000085)
19. Kilchoer C, Steiner U, Wilts BD. 2019 Thin-film structural coloration from simple fused scales in moths. *Interface Focus* **9**, 20180044. (doi:10.1098/rsfs.2018.0044)
20. Vanthournout B, Rousaki A, Parmentier T, Janssens F, Mertens J, Vandenabeele P, D'Alba L, Shawkey M. 2021 Springtail coloration at a finer scale: mechanisms behind vibrant collembolan metallic colours. *J. R. Soc. Interface* **18**, 20210188. (doi:10.1098/rsif.2021.0188)
21. D'Alba L, Saranathan V, Clarke JA, Vinther JA, Prum RO, Shawkey MD. 2011 Colour-producing beta-keratin nanofibres in blue penguin (*Eudyptula minor*) feathers. *Biol. Lett.* **7**, 543–546. (doi:10.1098/rsbl.2010.1163)
22. Gundersen H, Thaulow C, Leinaas HP. 2015 Seasonal change in the wetting characteristics of the cuticle of the Collembola *Cryptopygus clavatus* (Schott, 1893). *Zoomorphology* **134**, 211–218. (doi:10.1007/s00435-015-0254-y)
23. Schneider CA, Rasband WS, Eliceiri KW. 2012 NIH Image to ImageJ: 25 years of image analysis. *Nat. Methods* **9**, 671–675. (doi:10.1038/nmeth.2089)
24. Leertouwer HL, Wilts BD, Stavenga DG. 2011 Refractive index and dispersion of butterfly chitin and bird keratin measured by polarizing interference microscopy. *Opt. Express* **19**, 24 061–6. (doi:10.1364/OE.19.024061)
25. Stavenga DG, Leertouwer HL, Hariyama T, De Raedt HA, Wilts BD. 2012 Sexual dichromatism of the damselfly *Calopteryx japonica* caused by a melanin-chitin multilayer in the male wing veins. *PLoS ONE* **7**, e49743. (doi:10.1371/journal.pone.0049743)
26. Berenger JP. 1994 A perfectly matched layer for the absorption of electromagnetic-waves. *J. Comput. Phys.*. **114**, 185–200. (doi:10.1006/jcph.1994.1159)
27. Maia R, Eliason C, Bitton P, Doucet S. 2013 Shawkey M. pavo: an R package for the analysis, visualization and organization of spectral data. *Methods Ecol. Evol.* **4**, 906–913.
28. RStudio Team. 2021 *RStudio: integrated development environment for R*. Boston, MA: RStudio.
29. Gisin H. 1960 *Collembolenfauna Europas*. Geneva, Switzerland: Museum d'Histoire Naturelle.
30. Wolff JO, Schoenhofer AL, Schaber CF, Gorb SN. 2014 Gluing the 'unwettable': soil-dwelling harvestmen use viscoelastic fluids for capturing springtails. *J. Exp. Biol.* **217**, 3535–3544. (doi:10.1242/jeb.108852)
31. Delhey K. 2019 A review of Gloger's rule, an ecogeographical rule of colour: definitions, interpretations and evidence. *Biol. Rev.* **94**, 1294–1316. (doi:10.1111/brv.12503)
32. Wise DH. 2004 Wandering spiders limit densities of a major microbi-detritivore in the forest-floor food web. *Pedobiologia* **48**, 181–188. (doi:10.1016/j.pedobi.2003.12.001)
33. Baulechner D, Jauker F, Wolters V. 2022 Carabid adaptation to a collembolan diet: hunting efficiency and nutritional value. *Ecol. Entomol.* **47**, 242–248. (doi:10.1111/een.13106)
34. Salmon S, Geoffroy JJ, Ponge JF. 2005 Earthworms and collembola relationships: effects of predatory centipedes and humus forms. *Soil Biol. Biochem.* **37**, 487–495. (doi:10.1016/j.soilbio.2004.08.011)
35. Bauer T, Kredler M. 1993 Morphology of the compound eyes as an indicator of life-style in carabid beetles. *Can. J. Zool.* **71**, 799–810. (doi:10.1139/z93-105)
36. Hensel R, Neinhuis C, Werner C. 2016 The springtail cuticle as a blueprint for omniphobic surfaces. *Chem. Soc. Rev.* **45**, 323–341. (doi:10.1039/C5CS00438A)
37. Kim JH, Moon JH, Lee SY, Park J. 2010 Biologically inspired humidity sensor based on three-dimensional photonic crystals. *Appl. Phys. Lett.* **97**, 103701. (doi:10.1063/1.3486115)
38. Feng R, Song F, Xu C, Wang XL, Wang YZ. 2021 A quadruple-biomimetic surface for spontaneous and efficient fog harvesting. *Chem. Eng. J.* **422**, 130119. (doi:10.1016/j.cej.2021.130119)
39. Vanthournout B, Janssens F, Debruyn G, Mertens J, Clerck KD, D'Alba L, Shawkey M. 2023 Rapid and reversible humidity-dependent colour change by water film formation in a scaled springtail. Figshare. (doi:10.6084/m9.figshare.c.6845532)